Astron. Astrophys. 233, 583–597 (1990)

ASTRONOMY AND ASTROPHYSICS

Structure of solar magnetic fluxtubes from the inversion of Stokes spectra at disk center

C.U. Keller[1], S.K. Solanki[2], O. Steiner[1], and J.O. Stenflo[1]

[1] Institute of Astronomy, ETH-Zentrum, CH-8092 Zürich, Switzerland
[2] Department of Applied Mathematics, University of St. Andrews, St. Andrews KY16 9SS, Scotland

Received September 28, accepted November 7, 1989

Abstract. We present an inversion procedure that derives the temperature stratification, the turbulent velocity, and the magnetic field strength of the photospheric layers of small-scale magnetic fields from observed Stokes V spectra and the continuum intensity. The inversion is based on the determination of a small number of model fluxtube parameters by a non-linear least squares fitting algorithm. One-dimensional and two-dimensional fluxtube models are used to calculate synthetic Stokes V profiles, which are parameterized such that a given observable (a parameter that is extracted from the Stokes V profiles or from the continuum intensity) depends mainly on one particular model fluxtube parameter. The fluxtube models used take into account hydrostatic equilibrium, magnetic pressure, and magnetic flux conservation. The two-dimensional models also include magnetic tension and fluxtube merging. The minimization of the sum of the squared differences (χ^2) between observed and synthetic observables leads to a determination of the temperature stratification and the magnetic field strength, the main free parameters of the model fluxtube.

The inversion has been applied to high spectral resolution Fourier tranform spectrometer (FTS) observations of a plage and a network region located near disk center. 8 Fe I and 2 Fe II Stokes V line profiles between 5000 Å and 5500 Å are used, as well as the continuum contrast at 5000 Å. The temperature difference between the fluxtube interior and the quiet photosphere at equal geometrical height is found to decrease from an excess of 500–1000 K inside the fluxtubes in the upper photosphere to a deficit of about 2500 K at the level of continuum formation, in general agreement with the latest theoretical models. The application of the inversion procedure results in very similar temperature stratifications when using one-dimensional and two-dimensional fluxtube models. In agreement with earlier empirical models the fluxtubes in the network (smaller magnetic flux in the spatial resolution element) are found to be slightly hotter as compared with fluxtubes in active regions (larger magnetic flux). Furthermore we confirm that the magnetic field strength is approximately 2000–2300 G at the level of continuum formation and that the turbulent velocities are considerably larger in the fluxtubes than in the quiet photosphere. We also find that the field strength stratifications as a function of geometrical height in the plage and the network are practically indistinguishable from each other. Turbulent velocities, on the other hand are smaller in plage fluxtubes than in network fluxtubes.

Key words: solar magnetic fields – Stokes line profiles – fluxtubes – empirical models

Send offprint requests to: C.U. Keller

1. Introduction

Small-scale magnetic features called magnetic elements and often also called magnetic fluxtubes or facular elements, play an important role in our understanding of solar magnetic fields. Over 90% of the solar magnetic flux outside of sunspots is concentrated into small fluxtubes with a field strength greater than approximately 1000 G at the level of line formation (Howard and Stenflo, 1972; Frazier and Stenflo, 1972; Stenflo, 1973). Even sunspots possibly consist of a bundle of small fluxtubes (Parker, 1979; Spruit, 1981). Fluxtubes are the most likely channels for transporting the energy required to heat the solar corona and the upper chromosphere (e.g. Spruit and Roberts, 1983). It has been sugested that the lower chromosphere only exists within fluxtubes (Ayres and Testerman, 1981; Ayres et al., 1986). The small-scale magnetic elements probably affect the behavior of the global magnetic fields by their influence on the solar dynamo (Schüssler, 1983). They change the characteristics of the solar convection significantly (e.g. Title et al., 1989), and interact with solar p-modes (Bogdan and Zweibel, 1985; Bogdan and Cattaneo, 1989). Therefore, the temperature, magnetic field, and velocity stratifications within solar magnetic fluxtubes are essential for our understanding of solar and stellar activity.

Models of solar magnetic fluxtubes can be divided into two groups: empirical models derived from observations and theoretical models constructed from basic physical considerations without using observational data. We have grouped the so-called 'semi-empirical' models, obtained by fitting the free parameters of simple physically consistent models to observations, among the empirical models. Most published empirical fluxtube structures have been obtained by fitting synthetic spectra from simple fluxtube models to observed Stokes I line profiles of faculae (Chapman, 1977, 1979; Koutchmy and Stellmacher, 1978; Stellmacher and Wiehr, 1979; Walton, 1987), or by fitting the observed center-to-limb variations (CLV) of the continuum contrast of faculae (Rogerson, 1961; Chapman, 1970; Wilson,

1971; Muller, 1975; Hirayama, 1978). However, these attempts have failed in finding a unique model that explains the observations and is not heavily influenced by assumptions regarding the structure of the non-magnetic atmosphere between the fluxtubes. Because individual fluxtubes have so far not been resolved, any observation in unpolarized light will be subject to the mixing of information originating from magnetic and non-magnetic regions (see Solanki, 1990 for a detailed discussion of the shortcomings of models based on Stokes I only). Polarized light, on the other hand, originates exclusively in the magnetic parts of the atmosphere. The few models derived from Stokes V profiles, i.e. the difference between left and right circularly polarized spectra, (Stenflo, 1975; Solanki, 1984, 1986) have the substantial advantage that the analysis can be performed independently of the spatial resolution, and the results are not directly influenced by the poorly determined atmosphere surrounding the fluxtubes.

Therefore, we also use Stokes V spectra. The technique for deriving the fluxtube structure from them is based on the determination of a few model fluxtube parameters by a non-linear least squares algorithm. This approach is often referred to as an inversion. Fluxtube models that have the magnetic field strength, the temperature stratification, and the turbulent velocity structure as free parameters, but are otherwise self-consistent within the framework of magnetohydrodynamics, are used to calculate synthetic Stokes V profiles. The minimization of the sum of the squared differences between observed and synthetic observables (parameters that are extracted from the Stokes V profiles and the continuum intensity) leads to a determination of the free model parameters. The inversion procedure and the one-dimensional and two-dimensional magnetohydrostatic fluxtube models are described in Sect. 2. The inversion procedure has been applied to high quality Fourier transform spectrometer (FTS) data of a plage and a network region near disk center. Section 3 deals with these observational data and the spectral line selection. The success of such an inversion depends to a high degree on the availability of a set of observables, which respond in a sufficiently 'orthogonal' way to the various free parameters of the model. By appropriately choosing these observables the inversion procedure is accelerated and stabilized. The selected observables are described in Sect. 4. The fluxtube structures obtained by applying the inversion procedure to the FTS observations are presented in Sect. 5. Finally, Sect. 6 compares these empirical fluxtube models with previous models based on Stokes V data and with the latest theoretical fluxtube models that include a proper treatment of radiative energy transfer. Preliminary results of a part of the present investigations have been presented by Keller (1990).

2. Inversion of Stokes V data: description of technique and fluxtube models

The inversion of observed data to determine the free parameters of empirical models is often performed by minimizing the difference between observed and synthetic data using an iterative non-linear least squares algorithm. This was, for instance, done by Stenflo (1975) to derive his fluxtube temperature model from magnetograph recordings, and by Frazier and Stenflo (1978) to determine parameters characterizing the magnetic and velocity fields of the fluxtubes from Stokes V spectra. Inversion procedures have also been developed to derive vector magnetic fields from Stokes polarimeter observations (Auer et al., 1977; Skumanich and Lites, 1987), to obtain the sunspot temperature structure from Stokes I spectra (Van Ballegooijen, 1984), to derive temperature and velocity fluctuations in the chromosphere (Mein et al., 1985), and to produce models of umbral light bridges (Sobotka, 1989). We use the same efficient least squares algorithm (Marquardt, 1963) that has previously been used by Stenflo (1975) and Auer et al. (1977), and which requires only a small number of synthetic profile calculations. This is of extreme importance for our investigation because the fluxtube model calculations and the numerical solution of the transfer equations of polarized radiation need a large amount of computer resources.

The value that is minimized by the least-squares algorithm is defined by

$$\chi^2 = \frac{1}{\nu} \sum_{i=1}^{n} \frac{1}{\sigma_i^2} (R_i^o - R_i^s)^2 w_i^2, \tag{1}$$

where R_i^o are the observed and R_i^s the synthetic observables, σ_i the standard deviations of R_i^o, and w_i are the weights of the observables. These weights can be used to influence the inversion procedure, and to stabilize and accelerate the inversion. ν is the number of degrees of freedom, i.e. the difference between the number of observables and the number of free fluxtube model parameters. For $w_i = 1\ \forall i$ we expect χ^2 to be of the order of unity for a good fit, i.e., the average difference between the observed and fitted synthetic observables is of the order of one standard deviation of the observations. In general the weights are set to unity, but for observables that are excellent diagnostics for one particular fluxtube parameter they are doubled (magnetic line ratio and Fe I 5247.1 Å to Fe I 5250.7 Å ratio, see Sect. 4.3). They are reduced to 0.3 for observables that can only be marginally reproduced by the currently used fluxtubes models (ratio between two Fe II lines, see Sect. 4.2). This choice speeds up the inversion, but only marginally affects the resulting fluxtube models. All χ^2 values that are stated in this text are calculated with $w_i = 1\ \forall i$, whereas the minimization is carried out with the modified weights, which are the same for all models. For the particular choice of weights used in this work χ^2 with the modified weights is smaller than χ^2 with the weights set to unity and the difference between the two values is small. We feel that χ^2 obtained with $w_i = 1\ \forall i$ is the more reliable quantity to decide whether a fit is adequate or not.

Empirical models derived from observations should obey fundamental physical laws as encapsuled in, e.g., the magnetohydrodynamic (MHD) equations. This is ensured in the present investigation by the use of fluxtube models which represent static solutions of the MHD equations, excluding the energy equation, so that they do not a priori predict a temperature structure. We have made use of two such models. The simpler model is based on the thin tube approximation (see e.g. Roberts and Webb, 1978), i.e. it incorporates horizontal pressure balance (with the magnetic and gas pressure inside the fluxtube balancing the gas pressure outside the fluxtube) and hydrostatic equilibrium in the vertical direction. For the radiative transfer a single ray, corresponding to the axis of symmetry of the fluxtube, is chosen, i.e. the line profiles are calculated in a one-dimensional approximation. This does not account for the geometry of the fluxtube which flares out with height. We call models derived under these particular assumptions one-dimensional although the thin tube approximation is basically a two-dimensional model. The other model is constructed following Steiner et al. (1986), i.e. a cylindrically symmetric solution of the magnetohydrostatic equations is obtained. It takes into account the presence of a boundary current sheet, tension

forces, the merging of fluxtubes, as well as flux conservation. At the bottom of the computational grid we choose a horizontally homogeneous magnetic field distribution inside the tube and a sharp boundary at its edge, which is in good agreement with the internal magnetic field distribution derived from FTS infrared Stokes V spectra by Zayer et al. (1989). The model is used for multi-ray calculations, i.e. six vertical rays are passed through the model at various distances from its axis, along each of which the Stokes V profiles are calculated. All the profiles of a given line are finally weighted according to the surface area represented by each ray (corresponding to a ring in the cylindrical case) and added together to form an average profile, which is compared with the observations.

The free parameters of the models are the magnetic field strength at optical depth unity inside the fluxtube, $B(\tau_i=1)$, where subscript 'i' denotes the atmosphere inside the fluxtube, and the temperature as a function of the geometrical height $T(z)$. The zero level of the geometrical height scale corresponds to optical depth unity at 5000 Å of the quiet photosphere, $\tau_e=1$, where subscript 'e' designates the quiet solar atmosphere, which is assumed to surround the fluxtubes. Once these free model parameters have been prescribed or derived from the observations the rest of the model can be deduced from a solution of the magnetohydrostatic equations. The horizontally homogeneous temperature inside the fluxtube is given at seven grid points, at five of which, located at $z=300$, 100, 0, -100, and -200 km (corresponding to $\log\tau_i\approx -3.0$, -1.9, -1.1, -0.1, and 0.4 for the plage fluxtube structure that is described in Sect. 5.1), it is a free parameter. The temperature at the lowest point at -500 km is kept constant at 2000 K cooler than the quiet photosphere, as suggested by theoretical models (e.g. Deinzer et al., 1984a, b). Also, the difference between the temperatures inside the fluxtube and the quiet photosphere at the uppermost point (at $z=1200$ km) is kept the same as the temperature difference at the second highest grid point at 300 km. This ensures a smooth temperature stratification in the higher photospheric layers while avoiding the need to prescribe the temperature at the uppermost point outright. The precise choice of the upper 'boundary condition' does not influence the temperature stratification below the second highest grid point significantly. The temperature between the grid points is interpolated by cubic splines.

Since it is important to correctly reproduce the widths of the observed profiles, we must introduce non-stationary velocities both within and outside of the fluxtube. Following Solanki (1986) we make use of a combination of macro- and microturbulence velocities. Note that this does not imply the presence of true turbulence within the fluxtube. We use the simple turbulent velocity approach only as a tool to represent more complex motions. Detailed modelling of the Stokes V asymmetry has shown that the non-stationary velocities are probably due to waves or oscillations within the fluxtubes (Solanki, 1989). The microturbulent velocity in the fluxtube is assumed to have a height independent value of 0.6 km s^{-1} as in the quiet photosphere surrounding the fluxtubes. The macroturbulent velocity, $\xi_{\rm mac}$, on the other hand, is a free parameter for each spectral line. In order to reduce the number of free parameters the macroturbulent velocity is described as a function of the line strength S_I (defined as the area of the Stokes I profile below the half-level chord) and the effective excitation potential $\chi^\star$ via a regression equation. $\chi^\star$ is the sum of the excitation potential of the lower level of the transition and the ionization potential (7.87 eV in the case of neutral iron) if the line originates from an ionized atom (Dravins and Larsson, 1984). The regression equation has the form

$$\xi_{\rm mac}=a_1+a_2S_I+a_3S_I^2+a_4\chi^\star+a_5\chi^\star S_I, \qquad (2)$$

where a_i are the free parameters that are determined by the inversion procedure. This regression equation is roughly similar to the one used by Stenflo and Lindegren (1977) for the width of Stokes I profiles. However, Eq. (2) does not include a term proportional to the square of the effective Landé factor of the line because macroturbulent broadening must not compensate broadening due to the magnetic field. A regression approach has the added advantage that the correct $\xi_{\rm mac}$ can easily be calculated for any line, not only for the 10 lines used for the inversion in this investigation.

Extensive numerical tests have shown that the temperature at the level of continuum formation affects the stability of the inversion. However, recent publications (Grossmann-Doerth et al., 1988a; Rees et al., 1989) have shown that it is impossible to obtain information about the properties of fluxtube below $\log\tau_i\approx -1$ from Stokes V profiles in the visible, even when using the far wings of spectral lines, which are strongly affected by blends and noise. The continuum, however, is formed around $\tau_i=1$. By including continuum information we can better constrain the temperature stratification of the deeper layers of fluxtubes, and stabilize the inversion procedure. We use the continuum contrast at the axis of the fluxtube (i.e. the ratio of the continuum intensity at the axis of the fluxtube to that in the quiet sun), which requires data from extremely high spatial resolution observations.

Let us summarize the various steps of the program. We start with the prescribed initial values for the model parameters and calculate the corresponding fluxtube model. If the magnetic field is prescribed at a certain geometrical height the magnetic field stratification can be deduced consistently by solving the MHD equations. However, since the Stokes profiles are mainly sensitive to $B(\tau_i)$, it is advantageous to prescribe the field strength at a given optical depth. This requires the magnetic field strength to be changed iteratively at a certain geometrical height until $B(\tau_i=1)$ matches the prescribed value, because the magnetic field stratification changes the optical depth scale by modifying the gas pressure stratification inside the fluxtube. This method significantly accelerates the inversion, since it minimizes the change to the field strength at the optical depth of formation of a particular Stokes V profile, as the temperature structure evolves during the course of the inversion. Without this precaution any change in temperature 'felt' by the Stokes V profiles would be coupled to a sizeable change in the magnetic field via the dependence of the opacity on the temperature. For the two-dimensional model including magnetic tension $B(\tau_i=1)$ is determined from the thin tube approximation to save computer resources. This approximation is reasonable because at the layers of continuum formation the thin tube approach deviates only marginally from the exact solution of the MHD equations (see Knölker and Schüssler, 1988; Steiner and Pizzo, 1989). The continuum opacity is computed with the code of Gustafsson (1973). The Stokes profiles are calculated using the LTE code of Beckers (1969a, b), modified and extended by Solanki (1987). From these synthetic profiles the Stokes V observables and the continuum contrast are extracted and compared with the observations. To summarize, our inversion procedure thus makes use of 11 model parameters, one for

the magnetic field strength, 5 for the temperature stratification, and 5 for the macroturbulent velocity. The total number of observables (described in Sect. 4) is 31.

We face the problem of uniqueness of the solutions and of the sensitivity of the solutions to errors introduced by the measurements. We have tested the uniqueness of the derived fluxtube structures by starting the inversion procedure with widely different initial values for the free model parameters. When using 10 lines and 7 grid points for the temperature stratification we have always obtained the same final fluxtube structures within the accuracy of the program, which strongly supports the uniqueness of our solutions.

The errors in the derived structure ε_j introduced by errors in the measurements σ_i are defined by

$$\chi^2(b_1, \ldots, b_{j-1}, b_j+\varepsilon_j, b_{j+1}, \ldots, b_n) = \chi^2(b_1, \ldots, b_{j-1}, b_j, b_{j+1}, \ldots, b_n)+1, \quad (3)$$

where b_i are the optimum model parameters that have been found by the inversion, and ε_j is the value that must be added to a particular optimum model parameter b_j (while keeping the other optimum model parameters constant) such that χ^2 will increase by unity. The model parameters are normalized such that their optimum values b_i are of the order of unity. As mentioned above χ^2 of the optimum set of model parameters is of the order of unity. If ε_j is large compared with b_j the hyperplane χ^2 is flat with respect to the model parameter b_j, and the accuracy of b_j is poor. If ε_j is small the hyperplane χ^2 has a narrow minimum with respect to b_j and, therefore, the accuracy of the determination of b_j is high. ε_i can be calculated in a straightforward manner from the variance matrix of the inversion algorithm (e.g. Bevington, 1969). Henceforth we will call ε_i the external errors of the inversion routine. The internal errors, on the other hand, are produced by the inadequacy of the model itself, e.g. the assumption of a horizontally homogeneous temperature structure. Within the framework of the idealization made, a model can be considered to be fully successful if it uniquely fits the selected observables with a χ^2 of the order of unity. In fact, the derived fluxtube models show χ^2 values between 2.5 and 4.5, indicating that the model used is adequate to reproduce the data.

Our experience with codes of different levels of sophistication (e.g. different numbers of grid points and spectral lines) leads us to a rough estimate of the *internal* errors of the final code. They result in an uncertainty of 100 G in the magnetic field strength, of 200 K in the temperature stratification and of 0.3 km s^{-1} in the turbulent velocity. However, note that errors due to such assumptions as a horizontally constant temperature within the fluxtubes, or LTE are not quantifiable without substantially increasing the sophistication of the models or the radiative transfer. These internal errors are used when comparing the present models with other empirical or theoretical models which are derived under the assumption of LTE and do not exhibit significant horizontal temperature variations within the fluxtube. The external errors are generally much smaller than the internal errors and are therefore neglected. Typical values for the external errors are 50 K for the temperature, except for the highest regions of line formation where the external error can reach 200 K, 0.1 km s^{-1} for the macroturbulent velocity, and 10 G for the magnetic field strength. The small external errors suggest that the choice of observables used is adequate to determine the temperature, magnetic field, and turbulent velocity inside fluxtubes. Nevertheless the external errors of the network models exceed those of the plage models due to the smaller signal to noise ratio of the network Stokes V profiles. In particular they become the dominant source of uncertainty in the temperature of the upper photosphere of network fluxtubes.

3. Data and spectral lines

3.1. Observational data

We have applied the inversion procedure described in Sect. 2 to the FTS observations of Stenflo et al. (1984). The selected data consist of a plage and a network region near disk center that have been observed at a spectral resolution of 420'000 and with a circular entrance aperture having a diameter of 10 arcsec. The integration time was 35 min for the plage and 52 min for the network region giving a S/N ratio of 3000–10000 in the Stokes I continuum. The Stokes V profiles of the ten selected lines (see Sect. 3.2) have been anti-symmetrized around their zero-crossings, and the selected observables have been extracted. The errors in the observed Stokes V observables are determined more strongly by intrinsic effects due to the asymmetry of the Stokes V profiles (and possible blends) than by random noise (photon statistics), with the possible exception of the weakest lines. To account for this we let the standard deviations be given by

$$\sigma_i = \tfrac{1}{2}(|R_{i,\mathrm{red}}-R_i|+|R_{i,\mathrm{blue}}-R_i|), \quad (4)$$

where $R_{i,\mathrm{red}}$ and $R_{i,\mathrm{blue}}$ are the Stokes V observables extracted from the red, respectively blue wings of the original, asymmetric Stokes V profiles, and R_i are the Stokes V observables extracted from the antisymmetrized Stokes V profiles. This ensures that errors resulting from the anti-symmetrization of the Stokes V profiles are taken into account properly. The true continuum contrast on the axis of fluxtubes is not well determined by observations, but has been chosen to be 1.3 for the plage and 1.4 for the network region with a standard deviation of 0.1. These values are in approximate agreement with the observations of Muller and Keil (1983), and with the estimated lower limit of Schüssler and Solanki (1988) that is based on the same low spatial resolution FTS observations as used here. A slightly higher contrast for the network region as compared with the plage has been assumed, because fluxtubes in network regions are believed to be hotter than in plages. However, the continuum contrast remains a point of major uncertainty. Fortunately, small changes in I_c do not significantly affect $T(\tau_i)$ above $\log(\tau_i)\approx -1$, although unrealistically large values of I_c can alter the nature of the final solution even at the levels of line formation.

3.2. Spectral line selection and the model for the quiet photosphere

We have selected 8 Fe I and 2 Fe II lines in the range from 5000 to 5500 Å (see Table 1). 9 lines have been taken from the list of Solanki (1986), and Fe I 5250.7 Å has been chosen to form the thermal line ratio introduced by Stenflo et al. (1987). These lines are not or only slightly blended, they are formed in LS coupling, and they have been chosen to maximize the coverage of the plane formed by the line strength S_I and the effective excitation potential $\chi^\star$. Both the temperature sensitivity of lines and their heights of formation are governed by their strength and excitation potential, so that it is essential to cover the S_I vs. $\chi^\star$ plane when probing the temperature stratification of magnetic elements. Only

Table 1. Atomic parameters of the selected Fe I and Fe II lines

Ion	λ (Å)	χ_e (eV)	$g_{\text{eff}}^{\text{LS}}$	log gf (Thévenin)	log gf (this work)	S_I (F)	ξ_{mac} km s^{-1}	a_{mac}
Fe I	5048.4413	3.96	1.500	−1.20	−1.14	3.67	1.2	0.09
Fe I	5083.3450	0.96	1.250	−3.00	−3.15	6.70	2.1	0.03
Fe I	5127.6836	0.05	1.000	−6.06	−6.09	0.96	1.2	0.15
Fe II	5197.5742	3.23	0.700	−2.31	−2.65	4.33	1.0	0.05
Fe I	5247.0585	0.09	2.000	−4.97	−4.97	3.66	1.5	0.10
Fe I	5250.2171	0.12	3.000	−4.96	−4.92	3.69	1.35	0.19
Fe I	5250.6527	2.20	1.500	−2.01	−2.12	5.85	2.0	0.05
Fe I	5293.9609	4.14	1.000	−1.87	−1.68	1.44	1.7	0.03
Fe I	5383.3792	4.31	1.083	+0.48	+0.33	8.06	1.0	0.28
Fe II	5414.0736	3.22	1.206	−3.78	−3.70	1.45	1.9	0.05

few lines can be used due to the computational load imposed by the inversion technique, particularly for models with multiple lines of sight.

The log gf values (logarithm of the oscillator strength times the statistical weight of the transition) of these 10 lines have been determined by fitting FTS spectra from a quiet region at disk center (Stenflo et al., 1984) to a photospheric model, which is based on a combination of the empirical model of Vernazza et al. (1976, henceforth called VAL) and the theoretical convection zone model of Spruit (1977). Furthermore the temperature of the model for the quiet photosphere is required to be parallel to the Holweger-Müller model (1974) above the temperature minimum to provide a rough NLTE-masking (Rutten and Kostik, 1982). We thereby hide departures from LTE of Fe I caused by the presence of a chromosphere in the atmospheric model. By making the Planck function roughly similar to the source function of the cores of the strong Fe I lines we can reproduce the cores of these lines in LTE. By simultaneously fitting the Stokes I profiles of various spectral lines using the same code, the same observed spectrum, and a single atmospheric model of the quiet photosphere we eliminate the effects of discrepancies between various measurements of log gf, although we do not claim the derived log gf values to be correct on an absolute scale. Note that due to this procedure the fluxtube temperatures we derive are in a certain sense relative to the VAL atmosphere, since another quiet sun atmosphere would have given other log gf values. The microturbulent velocity of 0.6 km s^{-1} for the quiet photosphere has been assumed to be independent of height. The macroturbulent velocity distribution has the shape of a Voigt function $H(a_{\text{mac}}, \xi_{\text{mac}})$ (see Smith et al., 1976), where a_{mac} is the ratio of the damping to the Doppler width, and ξ_{mac} is the Doppler width of the macroturbulent velocity profile (see e.g. Mihalas, 1978). The resulting oscillator strengths, macroturbulent velocity parameters, and atomic line parameters are presented in Table 1 along with the empirical oscillator strengths obtained by Thévenin (1989). The wavelengths and the theoretical Landé factors of the lines in Table 1 have been taken from the lists of Solanki and Stenflo (1985), and the excitation potentials have been taken from Thévenin (1989). Our log gf determinations are in most cases in good agreement with the values determined by Thévenin, which are supposed to be free of systematic errors. The only significant deviation is found for Fe II 5197.6 Å, for which our determination of −2.65 seems to be too small. Moity (1983) found −2.35 and Kroll and Kock (1987) −2.10 for this Fe II line, which are in approximate agreement with −2.31 deduced by Thévenin. The iron abundance has been determined to be 7.42, which is in excellent agreement with 7.42 used by Thévenin, and derived by Holweger (1979) using the Holweger and Müller model (1974), but which is in slight contradiction to the measurements of Pauls et al. (1990), who found 7.66 ± 0.06. However, our abundance and oscillator strength determinations have not been performed for the purpose of obtaining accurate absolute values, but to find the values that establish consistency between our reference model atmosphere and observed FTS spectra. The deviations from the precision measurements have no significant influence on the resulting fluxtube structures since we use an essentially differential approach.

4. Selected observables

The speed of convergence and the uniqueness of the solution of the iterative fit algorithm described in Sect. 2 are determined by the way in which the comparison between observed and synthetic Stokes V profiles is performed. In the ideal case a set of 'orthogonal' observables is extracted from the observed profiles such that each of the corresponding synthetic observables depends on only one fluxtube model parameter. By orthogonal Stokes V parameters we mean that no two Stokes V parameters depend on one and the same fluxtube model parameter. Due to the extremely non-linear response of spectral line profiles to changes in the model parameters, it is not possible to find an ideal set of observables. However, it is possible to find certain observables that are much closer to being 'orthogonal' to each other than just the Stokes V profile values at various wavelengths.

It is important to parametrize the Stokes V profiles such that the observables can, in principle, be reproduced by the chosen model; otherwise the inversion procedure attempts to reproduce observed features that cannot be explained by the model; an example is the Stokes V asymmetry. Although the observed Stokes V asymmetry can be explained by the presence of stationary velocity fields in the non-magnetic surrounding atmosphere of the fluxtubes when combined with non-stationary velocities inside the fluxtubes (van Ballegooijen, 1985; Grossmann-Doerth et al., 1988b; Solanki, 1989), we anti-symmetrize all observed Stokes V profiles around their zero-crossing by taking the arithmetic mean of the blue and the red Stokes V wings. This

allows us to use simple magnetohydrostatic fluxtube models, which can only reproduce antisymmetric Stokes V profiles, instead of stationary or more complicated dynamic models.

4.1. *A grid of fluxtube models for numerical experiments*

To evaluate different choices of Stokes V observables to be used for the inversion, we have computed a grid of fluxtube model atmospheres by varying the free model parameters (temperature, magnetic field strength, turbulent velocities). The fluxtube model used for these exploratory calculations is based on the thin tube approach, according to which the magnetic field strength stratification is given by exact pressure balance. We have produced a grid of such models, which we describe below. The models in this grid are related to a standard fluxtube model which has a magnetic field strength of 2000 G at internal optical depth unity and a temperature stratification equal to that of the quiet photosphere at equal geometrical height. Nevertheless, the temperature at equal optical depth is approximately 2000 K hotter inside the fluxtube at the level of continuum formation due to the reduced opacity which, in turn, is a consequence of the horizontal pressure balance. A height-independent microturbulent velocity of 0.8 km s^{-1} is assumed, and the macroturbulent velocity distribution has a Gaussian profile with a Doppler width of 2.0 km s^{-1}. These values are in agreement with the empirical results of Solanki et al. (1987).

A first set of fluxtube models has height-independent temperature differences, ΔT, between the fluxtube interior and the quiet photosphere at equal geometrical height. The mean molecular weight is assumed to be the same inside the fluxtube and in the quiet photosphere at equal geometrical height throughout this work. This is a reasonable assumption since the variation of the mean molecular weight is extremely small when going from the deepest to the highest photospheric layers. ΔT ranges from -1000 K to $+1000$ K. We have investigated the influence of the fluxtube temperature structure on the emerging Stokes V profiles with these models. The magnetic field strength is adjusted such that $B(\tau_i=1)$ remains at 2000 G. This ensures that the magnetic field strength at the level of line formation remains approximately constant for different ΔT.

Since an increase in the field strength decreases the gas pressure at a given height the opacity decreases, so that the temperature as a function of optical depth, $T(\tau)$, also changes (although $T(z)$ remains unaffected). Therefore, changing the magnetic field strength consistently in a thin tube model has nearly the same influence on the Stokes V profiles as changing the temperature stratifications while keeping the magnetic field strength constant (cf. Steiner and Pizzo, 1989). To study the effects of various magnetic field strengths on the selected observables we have constructed another set of fluxtube models in which the magnetic pressure is not balanced by the gas pressure. They have the same temperature and gas pressure structure as a function of optical depth as the quiet photosphere, but include a magnetic field. Hence the temperature as a function of optical depth of this set of models is different from the one of the standard model. The height dependence of the magnetic field structure is taken from thin tube solutions with various $B(\tau_i=1)$, i.e. in the interest of understanding the diagnostic we artificially decouple the magnetic and thermodynamic parameters of the atmosphere.

The line profiles used to explore the influence of macroturbulence have been computed with the standard fluxtube model (with a microturbulent velocity of 0.8 km s^{-1}). Macroturbulent velocities of up to 3.0 km s^{-1} have been tried and a Gaussian profile for the velocity distribution has been assumed (the values in km s^{-1} refer to the Doppler width of this Gaussian). Numerical experiments have shown that the influence of microturbulent velocities on the Stokes V profiles is small as compared with the other free parameters of the model fluxtube. We shall, therefore, discuss them no further.

The thin tube approximation as well as other theoretical fluxtube models are based on the assumption of vertical fluxtubes. Measurements indicate that fluxtube 'bundles' are often inclined with respect to the vertical by more than 10 degrees (Solanki et al., 1987), in spite of reasonable theoretical arguments against any inclination exceeding one degree (Schüssler, 1986; however, see also Schüssler, 1990). Numerical experiments have been performed by forcing the magnetic field vector of a one-dimensional model to have a non-vanishing angle with respect to the line of sight while changing neither the magnetic field strength stratification nor any other atmospheric parameter. We deduce from these calculations that an inclination of less than 20 degrees affects the shape of Stokes V profiles only marginally.

In Sects. 4.2 to 4.5 we present 30 Stokes V observables that have been selected from a total of over 100 candidates, and discuss their dependence on the different model fluxtube parameters using the grid of fluxtube atmospheres introduced above.

4.2. *Fe I to Fe II Stokes V area ratios*

The amplitude a_V and the area of one wing A_V of a Stokes V profile (see Fig. 1 for a description of the various Stokes V profile parameters) are approximately proportional to the filling factor, which is the fraction of the resolution element covered by strong magnetic fields. Therefore, absolute values of the Stokes V amplitudes or wing areas cannot be directly used to derive the temperature. Ratios between such parameters of two lines, on the other hand, are mainly sensitive to the temperature and also partly to the magnetic field strength and to differential velocity broadening. Furthermore, Fe II lines are rather insensitive to temperature as compared with Fe I lines due to their high effective excitation potential, so that ratios of Fe I to Fe II Stokes V profiles are good temperature diagnostics (cf. Solanki and Stenflo, 1985). The Stokes V wing areas have certain advantages compared to the amplitudes. Areas of Stokes V wings are generally less affected by noise and exhibit smaller asymmetry as compared with the Stokes V amplitudes, although they are more affected by blends. Their interpretation is more straightforward, since the area of one wing of a Stokes V profile is proportional to the depth of the I_V profile (Solanki and Stenflo, 1984). I_V is proportional to the integrated Stokes V profile and is a good approximation for the Stokes I profile emerging from the same fluxtube atmosphere but without a magnetic field. For the interpretation of our numerical experiments it is, therefore, sufficient to consider the behavior of the unpolarized Stokes I profiles. Finally, wing areas are much less sensitive to macroturbulent broadening than amplitudes (cf. Solanki and Stenflo, 1986; note that the instrumental profile acts in much the same manner as a macroturbulent velocity).

Thus the first observables that have been selected are the logarithmic ratios of the areas of the Stokes V wings of the Fe I lines to the Stokes V wing areas of the Fe II 5197.6 Å line defined by

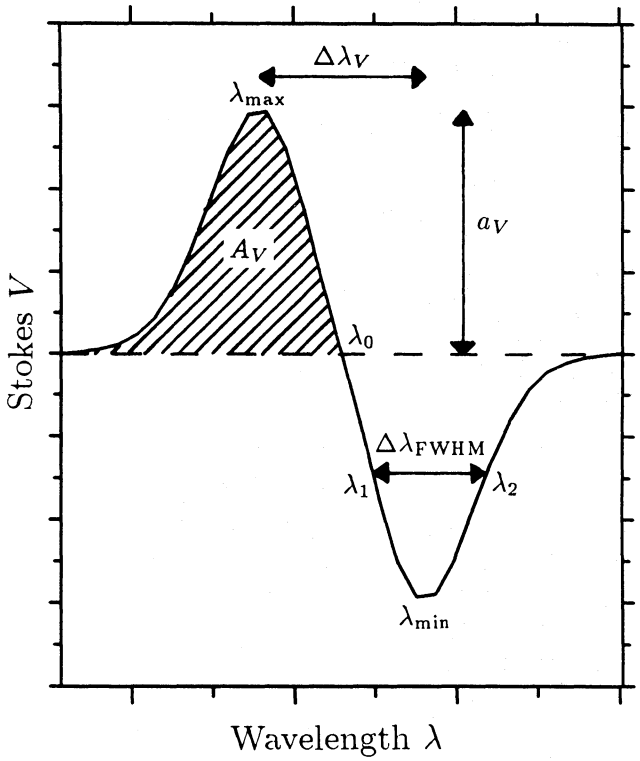

Fig. 1. An illustration of the parameters extracted from the observed Stokes V profiles. Note that most profile parameters are defined such that they can be determined independently for the red and the blue wing. a_V is the Stokes V amplitude, A_V the area of one Stokes V wing, λ_0 the zero-crossing of the Stokes V profile, λ_{max} and λ_{min} the wavelengths of the Stokes V profile maximum and minimum, respectively, $\Delta\lambda_V$ the Stokes V peak separation, and $\Delta\lambda_{FWHM}$ the full width at half maximum of one Stokes V wing

$$r_{I/II} = \log \frac{A_V(\text{Fe I})}{A_V(\text{Fe II } 5197.6\text{ Å})} . \quad (5)$$

Since strong Fe I lines are formed higher in the photosphere than weak Fe I lines, the temperature structure can be determined over different height ranges, by using Fe I to Fe II ratios with Fe I lines of different strength. In the present work we form the ratios of the Stokes V areas of Fe I 5048.4Å, Fe I 5083.3Å, Fe I 5127.7Å, Fe I 5247.1Å, Fe I 5250.7Å, Fe I 5294.0Å, Fe I 5383.4Å, and Fe II 5414.1Å, to that of Fe II 5197.6Å. In fact, the last ratio is formed between two Fe II lines, and Fe II 5414.1 is treated like an Fe I line. This ensures that the wing area of Fe II 5414.1 is fitted too, which is essential for an accurate determination of the macroturbulent velocity of this particular line. The remaining line (Fe I 5250.2Å) is not used, because this ratio would not be independent when simultaneously fitting the magnetic line ratio (see the next section).

The Stokes I line depth of moderately weak (e.g. Fe I 5247.1 Å) and weak (e.g. Fe I 5127.7 Å) Fe I lines decreases with increasing temperature, whereas Fe II lines are less affected. Therefore, the Fe I 5127.7 Å to Fe II 5197.6 Å Stokes V area ratio changes considerably with temperature (solid curve in Fig. 2). Strong Fe I lines (e.g. Fe I 5383.4 Å), on the other hand do not change their depths with increasing temperatures, although their widths decrease due to the smaller saturation at higher temperatures. Thus the Fe I 5383.4 Å to Fe II 5197.6 Å ratio remains almost constant (short dashes). Although this ratio cannot be used to determine the temperature in the higher regions of fluxtubes it must be fitted to reliably determine the macroturbulent velocity of this strong Fe I line. The influence of the magnetic field strength and of the macroturbulence are small as compared with the influence of the temperature (Fig. 2b, c). Note again that the temperature stratifications used to produce Figs. 2b and 2c are not the same. We conclude that the Stokes V Fe I to Fe II area ratios are excellent diagnostics for the temperature stratification of magnetic fluxtubes.

4.3. Ratios between Stokes V profiles of Fe I lines

Another observable we use is the well-known magnetic line ratio, i.e. the ratio of the Fe I 5247.1 Å to the Fe I 5250.2 Å Stokes V amplitudes divided by the ratio of the corresponding Landé factors (Stenflo, 1973; Stenflo and Harvey, 1985),

$$r_m = \frac{a_V(\text{Fe I } 5250.2\text{ Å})}{1.5\, a_V(\text{Fe I } 5247.1\text{ Å})} . \quad (6)$$

Because these two lines have nearly the same atomic parameters except for the Landé factor (see Table 1), their ratio is insensitive to all model fluxtube parameters except for the magnetic field strength at their height of formation, the macroturbulent velocity, and the angle of inclination. Extensive numerical experiments have already been carried out on this line ratio by Solanki et al. (1987) and Steiner and Pizzo (1989). They found that macroturbulent velocities have a large influence on the magnetic line ratio,

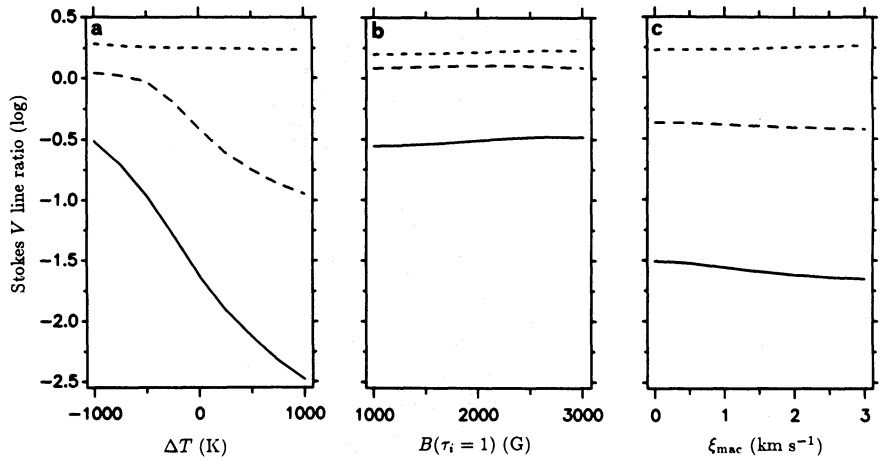

Fig. 2a–c. Logarithmic Stokes V area ratios: Fe I 5127.7 Å/Fe II 5197.6 Å (solid line), Fe I 5383.4 Å/Fe II 5197.6 Å (short dashes), and Fe I 5247.1 Å/Fe I 5250.7 Å (long dashes). See Sect. 4.1 for more details on the models used. **a** versus the temperature difference to the quiet photosphere at equal geometrical height ΔT, **b** versus the magnetic field strength at optical depth unity inside the fluxtube $B(\tau_i = 1)$, and **c** versus the macroturbulent velocity ξ_{mac}

and the angle of inclination has a considerable effect if it exceeds 20 degrees. The field strength is underestimated when turbulent velocities are neglected. Direct effects of the temperature structure are minute. For weak fields (Zeeman splitting much smaller than the Doppler width, i.e. a few hundred G for the sun) the ratio is unity, for stronger fields the ratio decreases monotonically with the magnetic field strength until it levels out close to 2/3 for sufficiently high field strengths. At even larger field strengths small changes in the line ratio still occur due to the non-triplet Zeeman splitting pattern of Fe I 5247.1 Å.

Harvey and Livingston (1969) first observed the weakening of Fe I 5250.2 Å with respect to Fe I 5250.7 Å in small magnetic features, but they did not explicitly form a line ratio. The Stokes V line ratio technique for the investigation of fluxtube temperature structures was introduced by Landi Degl'Innocenti and Landolfi (1982) in a theoretical context. Stenflo et al. (1987) used the Fe I 5247.1 Å and Fe I 5250.7 Å lines to form a thermal line ratio. These two lines have similar and not too large Landé factors (2.0 and 1.5, respectively) and similar line strengths in the quiet sun, so that they are affected by the magnetic field in much the same way. The difference in the excitation potential of their lower levels (0.09 eV as compared with 2.20 eV) gives rise to the substantial dependence of this line ratio on the thermodynamic properties of magnetic elements. We define the ratio as

$$r_t = \log \frac{A_V(\text{Fe I } 5247.1 \text{ Å})}{0.75\, A_V(\text{Fe I } 5250.7 \text{ Å})}, \tag{7}$$

where 0.75 is the ratio of the Landé factors. Although this ratio is not completely independent of the Fe I/Fe II ratios, it was felt that at least one temperature ratio not involving Fe II 5197.6 Å should be included.

The long-dashed curve in Fig. 2a shows the strong dependence of this thermal line ratio on the temperature stratification. The influence of the different Landé factors on the ratio is weak because none of the lines is significantly affected by Zeeman saturation for $B(\tau_i = 1)$ up to 3000 G (see Fig. 2b, long-dashed curve). The qualitative behavior of the two line ratios (magnetic and Fe I 5247.1 Å to Fe I 5250.7 Å) as a function of the macroturbulent velocity can be explained as follows: convoluting a spectral line with a Gaussian profile to account for the macroturbulence broadening is equivalent to low-pass filtering. Hence, the area A_V of a broad Stokes V profile is less influenced than the area of a narrow Stokes V profile. Fe I 5250.2 Å (due to the higher Landé factor) and Fe I 5250.7 Å (due to the larger line strength) have a broader Stokes V profile than Fe I 5247.1 Å. Therefore the magnetic line ratio increases and the Fe I 5247.1 Å to Fe I 5250.7 Å ratio decreases with increasing macroturbulent velocity. We conclude that the temperature derived from the latter line ratio alone is overestimated by up to 200 K when neglecting turbulent velocities (see Fig. 2c, long-dashed curve).

4.4. *Stokes V FWHM*

The inclusion of turbulent velocities is important for the determination of empirical fluxtube models, particularly for the determination of the temperature stratification (Solanki, 1986) and of the magnetic field strength (Solanki et al., 1987). To determine the macroturbulent velocity in fluxtubes we use the full width at half maximum (FWHM, in Å) of the Stokes V wings (see Fig. 1a)

$$\Delta\lambda_{\text{FWHM}} = \lambda_2 - \lambda_1. \tag{8}$$

For very low temperatures all lines are strong, and hence $\Delta\lambda_{\text{FWHM}}$ decreases with increasing temperature for all lines in this 'low' temperature regime (see Fig. 3a) due to partial removal of line saturation when ΔT is increased. However, only $\Delta\lambda_{\text{FWHM}}$ of the strong Fe I 5383.3 Å line (long dashes) decreases with increasing temperature in all temperature regimes, because this line is still strong at high temperatures. On the other hand, when lines become weaker they are formed deeper in the atmosphere, i.e. closer to the level of continuum formation and 'see' a higher magnetic field strength there. Therefore the Stokes V FWHM of lines with large Landé factors (e.g. Fe I 5250.2 Å, short dashes) increases with increasing temperature in regimes where the lines are weak. Magnetic broadening is seen in Fig. 3b, where we investigate the influence of the magnetic field strength on the FWHM. As expected $\Delta\lambda_{\text{FWHM}}$ increases steadily with increasing field strength. Fe I 5250.2 Å (short dashes) is completely split at higher field strengths, which leads to a fairly constant FWHM at high field strengths. The small decrease visible at high field strengths has probably to do with the fact that the field strength decreases with height. Increasing macroturbulent velocities increase the FWHM of all Stokes V profiles (Fig. 3c). Note that the tests of the diagnostics presented here are by no means exhaustive. For example, the temperature gradient also affects the FWHM significantly. However, with the exception of strong Fe I lines and lines with large Landé factors ($g > 2$), the Stokes V

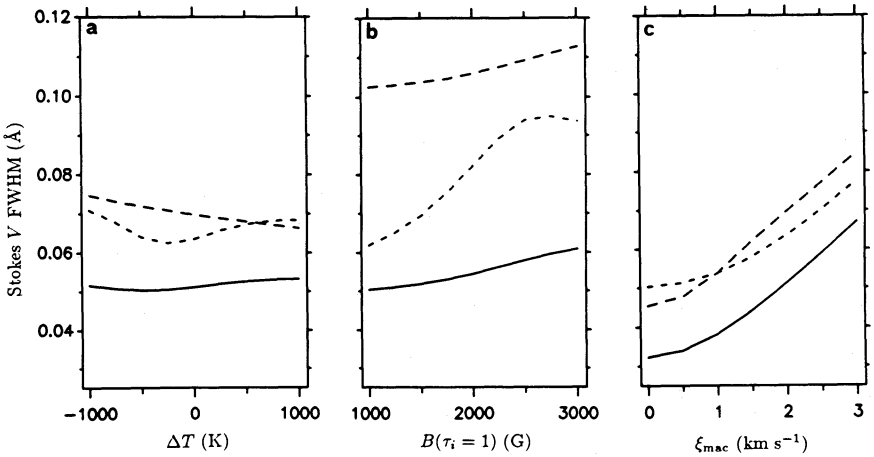

Fig. 3a–c. The FWHM (full width at half maximum, $\Delta\lambda_{\text{FWHM}}$ in Å) of the Stokes V wings of Fe I 5127.7 Å (solid line), Fe I 5250.2 Å (short dashes), and Fe I 5383.4 Å (long dashes) **a** versus the temperature difference to the quiet photosphere at equal geometrical height ΔT, **b** versus the magnetic field strength at optical depth unity inside the fluxtube $B(\tau_i = 1)$, and **c** versus the macroturbulent velocity ξ_{mac}

FWHM is sensitive almost exclusively to ξ_{mac}. For the strong Fe I lines there is no single clean diagnostic for ξ_{mac} available and this parameter must be determined in conjunction with the temperature.

4.5. *Stokes V peak separation*

The temperature in the higher photospheric layers of fluxtubes cannot be deduced from Fe I to Fe II ratios, because these observables are insensitive to temperature for strong Fe I lines formed in those higher layers (cf. Fig. 2a). Since Stokes I line widths of strong lines are sensitive to the temperature we expect the wavelength separation of the Stokes V extrema of strong lines to depend on the temperature as well (recall that $V \sim \partial I/\partial\lambda$). The Stokes V peak separation has been defined to correspond to the wavelength separation of the extrema of an antisymmetric Stokes V profile:

$$\Delta\lambda_V = 2|\lambda_{extr} - \lambda_0|. \quad (9)$$

As can be seen from Fig. 4, where the peak separation is plotted for the same lines and the same models as in Fig. 3, $\Delta\lambda_V$ behaves qualitatively similarly to the Stokes V FWHM. However, the dependence on temperature is more pronounced, as is the dependence on the the field strength of lines with large Landé factors. The sensitivity of $\Delta\lambda_V$ to ξ_{mac}, on the other hand, is smaller, in particular for the strong Fe I 5383.4 Å line (long dashes in Fig. 4c). By requiring both observables, $\Delta\lambda_{FWHM}$ and $\Delta\lambda_V$, to be simultaneously reproduced by the synthetic profiles we hope to be able to separate the influences of temperature and macroturbulence on strong Fe I lines and thus to determine both these quantities.

We caution that $\Delta\lambda_V$ alone allows a determination of the field strength only if the Zeeman splitting is much larger than the Doppler width (Fe I 5250.2 Å for $B(\tau_i = 1) > 2000$ G, Fig. 2b). For smaller Zeeman splittings $\Delta\lambda_V$ depends critically on other fluxtube parameters like temperature, the macroturbulence and the gradient of the field strength (see Fe I 5127.7 Å and Fe I 5383.3 Å in Fig. 4b. Note that $\Delta\lambda_V$ of the latter actually decreases with increasing field strength).

5. Results

5.1. *One-dimensional models*

The temperature stratifications obtained by applying the inversion procedure using the thin tube single ray model (cf. Sect. 2) to the FTS Stokes V spectra are presented in Fig. 5 for the plage (short dashes) and the network (long dashes) region (cf. Sect. 3.1) as a function of continuum optical depth at 5000 Å (Fig. 5a) and

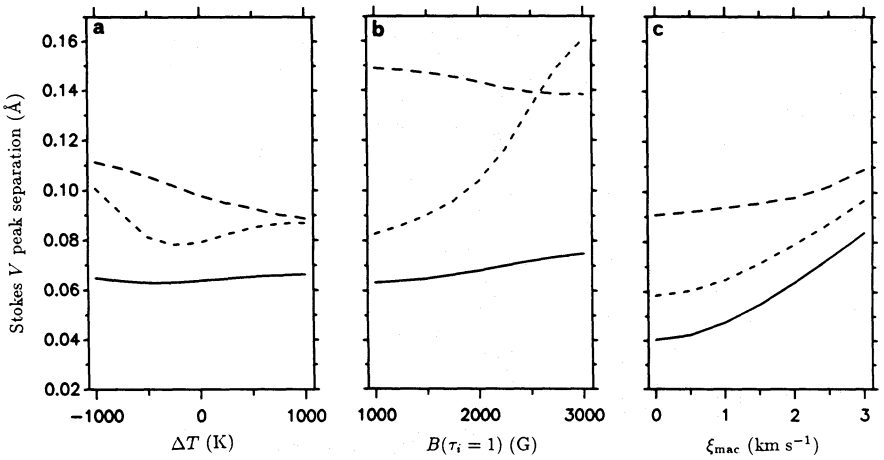

Fig. 4a–c. The Stokes V peak separation $\Delta\lambda_V$ in Å of Fe I 5127.7 Å (solid line), Fe I 5250.2 Å (short dashes), and Fe I 5383.4 Å (long dashes) **a** versus the temperature difference to the quiet photosphere at equal geometrical height ΔT, **b** versus the magnetic field strength at optical depth unity inside the fluxtube $B(\tau_i = 1)$, and **c** versus the macroturbulent velocity ξ_{mac}

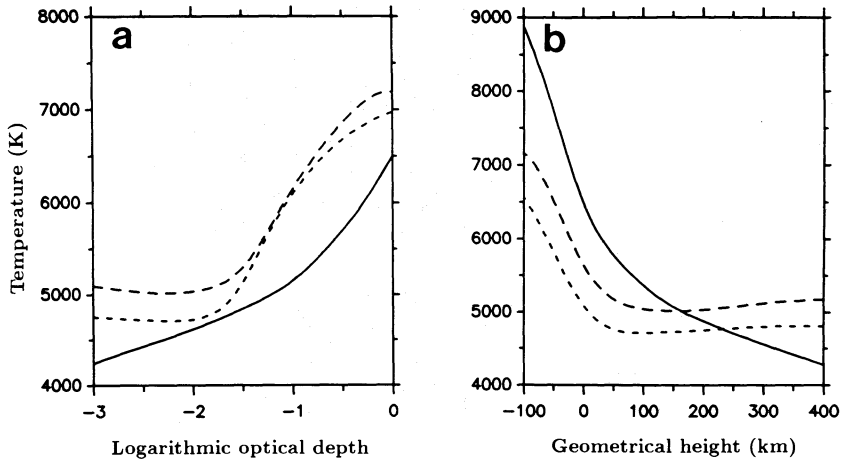

Fig. 5a and b. One-dimensional fluxtube models derived for the plage (short dashes) and the network region (long dashes), compared with the quiet photosphere (solid line). The 5 grid points used for the inversion are located at $z = -200$, -100, 0, 100, 300 km, which corresponds to $\log(\tau_i) = -3.9$, -1.9, -1.1, -0.1, 0.4 for the plage fluxtube model. **a** Temperature vs. continuum optical depth at 5000 Å, **b** temperature vs. geometrical height

geometrical height (Fig. 5b) along with the temperature stratification of the quiet photosphere (solid curve) has also been plotted. In general the fluxtubes are hotter than the quiet photosphere at all optical depths, although there is a marked dip around $\log \tau_i = -2$. At equal geometrical height we can distinguish two regions: below about 100–200 km fluxtubes are cooler than the quiet photosphere, above 200 km they are hotter. Note that the temperature inside the fluxtubes is nearly constant above 100 km. The network fluxtubes seem to be hotter than the plage fluxtubes everywhere, while the magnetic field strength is slightly larger in plage fluxtubes at equal optical depth (see Table 2 for a list of the magnetic field strengths, the macroturbulent velocities, and the χ^2 of the resulting models). While macroturbulent velocities are substantially larger inside fluxtubes than in the quiet photosphere (particularly for stronger lines), ξ_{mac} is smaller in plage fluxtubes as compared with network fluxtubes for all lines except for the very weak Fe I 5127.7 Å line, which is heavily affected by noise.

To obtain a feeling for the overall accuracy of the results we have performed several tests. Because this kind of inversion needs a large amount of computer resources, many exploratory calculations have been carried out with a reduced number of free model parameters and spectral lines, i.e., with three free grid points along the vertical axis and six spectral lines. From these tests we conclude that the choice of the grid point locations is not a critical one and that the present method of deriving the temperature structure of magnetic fluxtubes is not affected by the microturbulence if its velocity does not exceed 1.2 km s^{-1}. However, the temperature structure depends critically on the number of grid points. With 3 free grid points we can only marginally reproduce the stratification obtained with 5 free grid points. We feel that any further increase of the number of grid points would not change the results significantly although this has not been tested so far. A certain minimum number of spectral lines is also important for the derivation of a reliable stratification as a function of optical depth in two ways: 1) More lines cover the height range better (if they are properly selected) and hence constrain the temperature better. 2) The influence of noise, blends, etc. in the individual profiles has a smaller effect on the derived temperature structure.

The Fe II 5197.6 Å line plays a key role in the present work; advantageously the influence of any uncertainty in its oscillator strength on its line profile has been found to be weak. This is mainly due to the fact that this line is sufficiently strong for its depth to be practically unaffected by changes in $\log gf$. Fortunately the line depth is the most important parameter of this line (recall that the Stokes V wing area corresponds approximately to the depth of the Stokes I profile arising from the magnetic feature only). Although the temperature deficit of our magnetic fluxtube models of 2000 K at -500 km is in agreement with theoretical models (e.g. Deinzer et al., 1984b) models with a vanishing temperature difference at -500 km show no significant change in the derived temperature structure at the height of line formation. This is not surprising since the Stokes V profiles are not sensitive to the atmosphere below $\log \tau_i \approx -1$ in LTE. The assumption that the temperature difference at 1200 km is the same as at 300 km influences the shape of the temperature stratification above 300 km although the temperature at 300 km is barely affected.

5.2. *Two-dimensional models*

Although one-dimensional models are expected to be adequate for many aspects of disk center analyses (cf. Solanki, 1989) the exact influence of the radiative transfer along a single ray and of the thin tube approximation can only be explored by carrying out the inversion using full two-dimensional solutions of the MHD equations including radiative transfer along many rays, so that the spreading of the field with height (which assures the conservation of magnetic flux as seen by the spectral lines) is properly taken into account.

The computation of two-dimensional models requires prescription of the filling factor, which is determined by the radius of the fluxtube at a particular height and the distance between two adjacent fluxtubes. All models have been calculated with a radius of 100 km at $z=0$ and a distance between the axes of adjacent fluxtubes of 800 km, giving a filling factor of about 6% at $z=0$. Calculations with a radius of 200 km at $z=0$ and a filling factor of about 25% show that both the size and the filling factor of the fluxtube have a negligible influence on the derived temperature structure at disk center. Nevertheless the magnetic field as a function of geometrical height changes because the thicker tube reaches the height where it merges with adjacent fluxtubes lower

Table 2. Resulting fluxtube model parameters

	Plage 1-D	Network 1-D	Plage 2-D	Network 2-D	Units
$B(\tau_i=1)$	2360	2080	2370	2040	G
ξ_{mac}(Fe I 5054.4 Å)	1.9	2.3	1.9	2.1	km s^{-1}
ξ_{mac}(Fe I 5083.3 Å)	2.3	2.8	2.3	2.9	km s^{-1}
ξ_{mac}(Fe I 5127.7 Å)	1.4	1.1	1.5	0.8	km s^{-1}
ξ_{mac}(Fe II 5197.6 Å)	2.4	3.4	2.3	2.8	km s^{-1}
ξ_{mac}(Fe I 5247.1 Å)	1.7	1.9	1.8	1.7	km s^{-1}
ξ_{mac}(Fe I 5250.2 Å)	1.7	1.9	1.8	1.7	km s^{-1}
ξ_{mac}(Fe I 5250.7 Å)	2.3	2.8	2.2	2.6	km s^{-1}
ξ_{mac}(Fe I 5294.0 Å)	1.3	1.6	1.4	1.7	km s^{-1}
ξ_{mac}(Fe I 5383.4 Å)	3.2	3.6	3.0	3.3	km s^{-1}
ξ_{mac}(Fe II 5414.1 Å)	1.1	2.3	1.3	2.8	km s^{-1}
$\chi^2(\omega_i=1\,\forall i)$	3.5	2.5	4.0	4.2	—

in the atmosphere than the thinner tube; therefore its magnetic field strength is larger in the chromosphere.

Although Stokes V profiles are formed in magnetic regions only, their shape is also affected by the non-magnetic atmosphere whenever a single ray passes through both magnetic and non-magnetic regions (Van Ballegooijen, 1985; Grossmann-Doerth et al., 1988b). It is likely that the atmosphere surrounding the fluxtubes has a different temperature stratification than the quiet photosphere, as suggested by observations (e.g. Schüssler and Solanki, 1988; Solanki, 1989) and expected from theoretical model calculations (Spruit, 1977; Deinzer et al., 1984a, b; Grossmann-Doerth et al., 1989). We have also tested the influence of the surrounding atmosphere on the results of our inversion by decreasing its temperature by 1000 K. We do not observe a significant change in the resulting fluxtube structure, which is in accordance with the calculations of Solanki (1989).

The temperature and magnetic field stratifications obtained using two-dimensional fluxtube models are plotted in Fig. 6 versus the optical depth (Fig. 6a, c) and the geometrical height (Fig. 6b, d). The difference between the temperature structures of two-dimensional and one-dimensional models is small. The resulting macroturbulence velocities and the magnetic field strengths at $\tau_i = 1$ (see Table 2) are also similar. Even the synthetic Stokes V profiles do not show any significant differences between one-dimensional and two-dimensional models (short- and long-dashed curves, respectively in Fig. 7; the solid curves are the antisymmetrized observed profiles). Although there is a difference of about 300 G between $B(\tau_i = 1)$ of the plage (short dashes in Fig. 6c) and the network fluxtube (long dashes) the difference between the corresponding magnetic field stratifications at equal geometrical height is remarkably small (Fig. 6d). We conclude that the substantial difference of the $B(\tau_i = 1)$ values between plage and network fluxtubes is mainly due to the different temperature structures. Due to their lower temperature the plage fluxtubes have a lower continuum opacity, allowing light from deeper within them (where the field strength is larger) to escape (Schüssler, 1987).

The behavior of $T(z)$ or $T(\tau_i)$ near $\tau_i = 1$ within the fluxtube should not be taken too literally, since there is only a single observational data point below $\log \tau_i = -1$ to constrain the temperature stratification, namely the continuum contrast. It restricts the average temperature near $\tau_i = 1$, but not the detailed temperature stratification. An additional uncertainty in $T(\tau_i)$ is introduced by the uncertainty in the continuum contrast itself. Bearing this and other constraints in mind, we feel that the present fluxtube models are reliable only within the range $-3 \lesssim \log \tau_i \lesssim -1$.

6. Discussion

We have derived empirical models of the atmosphere and the magnetic field within magnetic elements from Stokes V profiles

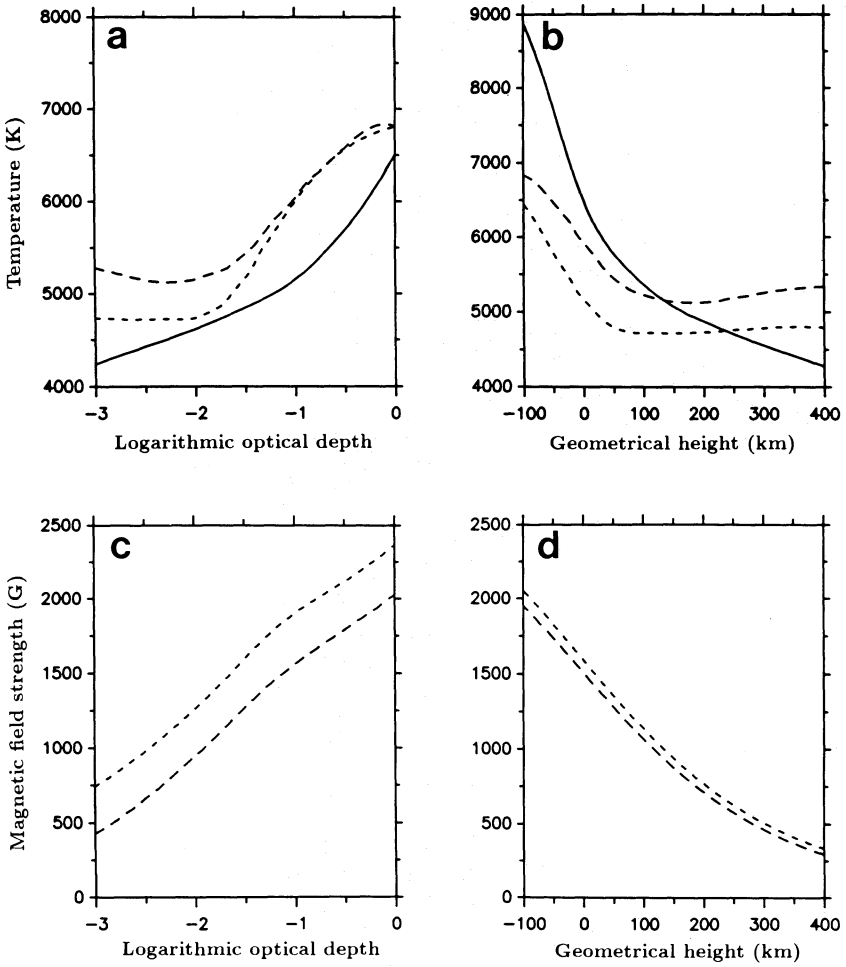

Fig. 6a–d. Two-dimensional fluxtube models for the plage (short dashes) and the network region (long dashes), compared with the quiet photosphere (solid line). **a** Temperature on the axis vs. optical depth, **b** temperature on the axis vs. geometrical height, **c** magnetic field strength on the axis vs. optical depth, **d** magnetic field strength on the axis vs. geometrical height

using an inversion technique. We now discuss the results by comparing them with other empirical and with theoretical fluxtube models. Later we consider possible shortcomings of the present approach and look to the future.

Although many models of the fluxtube temperature stratification have been derived in the past, only the results of Stenflo (1975) and Solanki (1984, 1986) can be compared with our temperature stratifications, because they have also been derived from Stokes V data. Indeed, the results of Solanki (1986; dot-dashed curve in Fig. 8a) are very similar to the present ones (short dashes). We do not think that the differences are significant, since the maximum difference between the two models corresponds to 200–300 K, which is comparable to the uncertainty in the derived temperatures of the individual models (see Sect. 2). Some of the differences might even be due to the different quiet sun models used, since Solanki (1986) derived the temperature stratification with respect to the HSRA (Gingerich et al., 1971). This similarity of the two models derived from the same data, but using different approaches, is very encouraging. The earlier inversion work of Stenflo (1975; long dashes) was based on a very limited data set (essentially two Stokes V line ratios), and constrained the temperature variation with optical depth through an analytical function, to limit the number of free parameters and make the inversion problem tractable at that time. This and the low continuum contrast assumed by Stenflo (which was in line with the then generally accepted value) accounts for the difference between his and our results. Further details on the comparison of various fluxtube models based on Stokes V may be found in Solanki (1990).

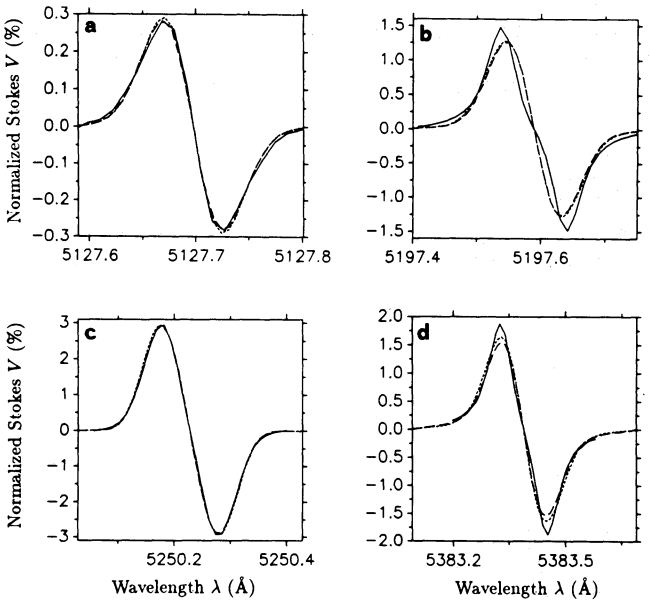

Fig. 7a–d. Synthetic Stokes V profiles from the one-dimensional (short dashes) and the two-dimensional (long dashes) plage fluxtube models compared with the anti-symmetrized observed Stokes V profiles (solid line) of the plage data. Note that the Stokes V amplitudes have not been fitted, which partly explains the difference between observed and synthetic profiles. **a** Fe I 5127.7 Å, **b** Fe II 5197.6 Å, **c** Fe I 5250.2 Å, **d** Fe I 5383.4 Å

Fluxtubes in the network region are found to be hotter than those in plages at equal optical depth as well as at equal geometrical height (see Fig. 6a, b) in agreement with earlier empirical models (Solanki, 1986). Two mechanisms for producing this temperature difference have been proposed. Fluxtubes in plages may be less efficiently heated than those in the network due to their larger diameter (e.g. Knölker et al., 1985; Knölker and Schüssler, 1988), or due to their larger number density in active regions (Schüssler, 1987). A combination of the two effects is also a distinct possibility. The smaller temperature and turbulent velocity found in plage fluxtubes with respect to the network fluxtubes is consistent with the dependence of the intrinsic fluxtube structure on the filling factor observed by Stenflo and Harvey (1985), Solanki (1986), and Pantellini et al. (1988).

The present fluxtube models are cooler than the quiet photosphere below $z=0$ km. Since Stokes V profiles are formed as low as $z=0$ km inside the fluxtubes, due to the shifted optical depth scale there (Wilson depression), the temperature deficit is not solely due to the assumption of a particular value for the continuum contrast of magnetic fluxtubes but is mainly based on observed spectral lines. The inhibition of convective motions within magnetic elements is likely to be the source of this temperature deficit (cf. Biermann, 1941; Spruit, 1976). In Fig. 8b the two currently most sophisticated theoretical models, those of Grossmann-Doerth et al. (1989, dot-dashed curve) and of Steiner and Stenflo (1990, long-dashed curve) are plotted together with the present plage (short dashed curve) and network (dotted curve) models and the quiet sun atmosphere (solid curve). Deinzer et al.

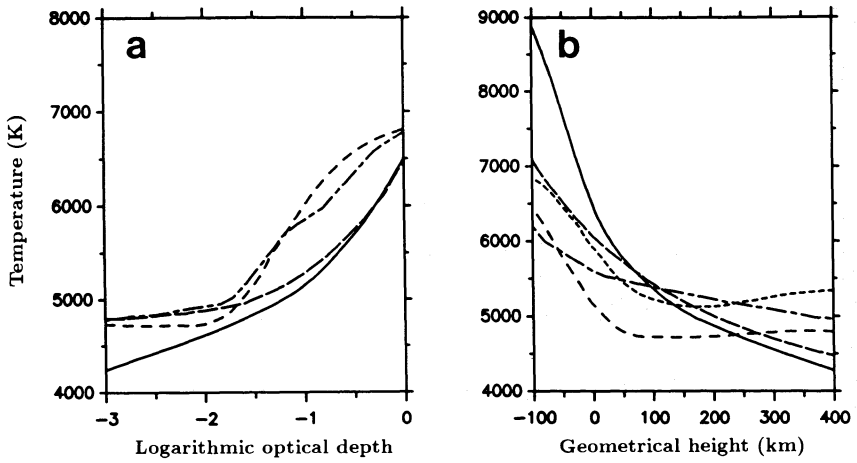

Fig. 8. a Comparison between the temperature structures at equal optical depth of the two-dimensional empirical plage fluxtube model (short dashes) of the present work, the fluxtube model of Stenflo (1975, long dashes), the one-dimensional empirical plage fluxtube model of Solanki (1986, dashed-dotted line), and the quiet photosphere (solid line); **b** Comparison between the temperature structures at equal geometrical height of the two-dimensional empirical plage (short dashes) and network (dotted line) fluxtube models of the present work, the two-dimensional theoretical model of Grossmann-Doerth et al. (1988a, dashed-dotted line), and the two-dimensional theoretical fluxtube model of Steiner and Stenflo (1990, long dashes)

(1984a, b) found a temperature deficit of up to 3000 K at $z = -125$ km in their theoretical models, which is in good agreement with our results. The temperature excess observed in the higher layers of our empirical models and the theoretical models (see Fig. 8b) has been explained by radiative transfer effects. The hot bottom (i.e. the $\tau_i = 1$ region) illuminates and heats the higher levels of the fluxtubes (Kalkofen et al., 1989; Grossmann-Doerth et al., 1989; Steiner and Stenflo, 1990). Note, however, that the $T_i(z)$ of the only theoretical model with a non-grey radiative transfer (Steiner and Stenflo, 1990; cf. Steiner, 1990, for more details) lies below the empirical curves above $z \approx 270$ km. Since the Steiner and Stenflo model is in radiative equilibrium, this suggests that mechanical heating may be important within fluxtubes in the middle and upper atmosphere.

Although there is general agreement between theoretical and empirical models, we want to emphasize that existing theoretical models do not predict the bend in the temperature structure occurring around $\log(\tau_i) = -2$ in the empirical models. In particular the plage model exhibits an unexpected low temperature there. There are various possible reasons for this discrepancy between theoretical and empirical models. The first is that the theoretical fluxtube models may not include all the physics relevant to the lower photosphere. In particular the best current theoretical fluxtube models of magnetic elements do not explicitly take into account that magnetic elements are preferably located in intergranular lanes. This would reduce the amount of radiation emerging laterally through the walls into the fluxtube at or below $\tau_e = 1$, and thus lead to a cooling of the tube. Also, current theoretical models always consider lone fluxtubes, whereas in reality fluxtubes often occur in groups. The difference may, however, simply be due to a choice of diameters of tubes in the theoretical models not corresponding to those in the observed regions. Yet another possibility has to do with the field strength. We wish to point out that the $T(z)$ derived from the data depends on the field strength, since the Stokes V profile ratios primarily give $T(\tau_i)$. If the field strength at $\tau_i = 1$ is wrong by even a few hundred Gauss, this will affect the $T(z)$ significantly. However, we feel that $B(\tau_i)$ should be certain to within approximately 150 G. Note that the B value derived here is consistent with the value obtained from very sensitive infrared data by Zayer et al. (1989).

Another possibility for the discrepancy is related to our data set. Due to the long integration time and the moderate spatial resolution of the FTS observations the derived fluxtube temperature stratifications represent some kind of statistical average over an ensemble of fluxtubes and might not correspond to any real stratification at a given moment in time. This is a basic limitation of the data set we have used and the question of how strongly the temperature fluctuates from one fluxtube to another can only be resolved with new high spatial resolution observations. In addition, if the radius of a fluxtube exceeds the local photon mean free path, then horizontal temperature inhomogeneities within a single fluxtube are possible. Although we have calculated two-dimensional models, we have assumed the temperature to be horizontally constant within the tube (to avoid introducing additional free parameters). The breakdown of this assumption or the presence of fluxtubes with different temperatures in the resolution element would cause spurious structures in the vertical temperature stratification by the inversion procedure. At present it is difficult to say how much of the structure in the derived $T(z)$ stratification is real, and how much is due to such effects. However, tighter limits have been set on possible variations of the magnetic field strength from one fluxtube to another by Zayer et al. (1989). If there were a statistical spread of fluxtube magnetic field strengths within the spatial and temporal resolution element, or a significant distribution of field strengths horizontally across the fluxtubes, this would give rise to Stokes V line broadening effects in the infrared, in contradiction with observations (Zayer et al., 1989). Further observational arguments for the 'uniqueness' of some aspects of the structure of fluxtubes have been given by Stenflo (1976, 1989).

It is rather difficult to estimate the influence of possible errors and idealizations on the derived fluxtube structures. The small set of grid points and lines, the assumption of horizontally homogeneous temperature structures, LTE, and the continuum contrast values are probably the most severe limitations of the present work. We feel that the combined microturbulence and macroturbulence approach, the neglect of the angle between the magnetic field and the vertical, and the anti-symmetrization of the Stokes V profiles play only a minor role. Reliable observations of the continuum contrast at disk center are sorely needed to empirically probe the lower layers of the fluxtubes. One possibility is to use Stokes V profiles formed near 1.6 μm, in the opacity minimum, however, unfortunately all the reliably identified iron lines in that stretch of the spectrum have very similar excitation potentials over 5 eV (Solanki et al., 1990), thus making the use of an inversion procedure as developed here impractical.

Although we have not included NLTE effects in the present calculations, the sun probably does not neglect them. For various fluxtube models (none of which possessed a chromospheric temperature rise) Solanki and Steenbock (1988) showed that NLTE effects are larger than for the quiet sun. In general their calculations imply that temperatures derived in LTE are somewhat overestimated. The same basic result was also found by Stenholm and Stenflo (1978), who showed that in a two-dimensional fluxtube model with hot walls (i.e. deep in the photosphere) lines could be significantly weakened by NLTE effects, even if the temperature within the fluxtube were only as high as in the quiet photosphere at equal optical depth. Note, however, that our models suggest that this last mechanism is not expected to be very important, since the low excitation Fe I lines, which are most susceptible to NLTE weakening, are formed at a height at which the fluxtube is either at a similar or higher temperature than its surroundings.

We expect one major exception to the conclusion that the neglect of NLTE effects leads to an overestimate of the temperature in the fluxtube. If the chromospheric temperature rise were to occur in fluxtubes already in the upper photosphere, then no significant effect is expected to be seen in the strong Fe I lines whose cores are formed at this height, since the source function in the core of such a line is largely decoupled from the Planck function. Therefore, an early chromospheric temperature rise is not expected to be reflected in LTE models like ours. A full NLTE treatment is required to resolve this problem.

For future work it would be most useful to include the center to limb variation of the continuum contrast and the Stokes line profiles into the inversion procedure. As we have seen above the geometry of the fluxtube cannot be determined from disk center data alone. However, observations obtained near the limb are sensitive to the geometry of the fluxtubes, as shown by Zayer et al. (1989). In addition the Stokes Q relative area asymmetry (cf. Solanki et al., 1987) can be used as a further temperature diagnostic.

Acknowledgements. CUK and OS wish to acknowledge the support by the Swiss National Science Foundation under grant No. 2000-5.229.

References

Auer, L.H., Heasley, J.N., House, L.L.: 1977, *Solar Phys.* **55**, 47
Ayres, T.R., Testerman, L.: 1981, *Astrophys. J.* **245**, 1124
Ayres, T.R., Testerman, L., Brault, J.W.: 1986, *Astrophys. J.* **304**, 542
Beckers, J.M.: 1969a, *Solar Phys.* **9**, 372
Beckers, J.M.: 1969b, *Solar Phys.* **10**, 262
Bevington, P.R.: 1969, *Data Reduction and Error Analysis for the Physical Sciences*, McGraw-Hill, New York
Biermann, L.: 1941, *Vierteljahrssch. Astron. Gesellsch.* **76**, 194
Bogdan, T.J., Cattaneo, F.: 1989, *Astrophys. J.* **342**, 545
Bogdan, T.J., Zweibel, E.G.: 1985, *Astrophys. J.* **298**, 867
Chapman, G.A.: 1970, *Solar Phys.* **14**, 315
Chapman, G.A.: 1977, *Astrophys. J. Suppl. Ser.* **33**, 35
Chapman, G.A.: 1979, *Astrophys. J.* **232**, 923
Deinzer, W., Hensler, G., Schüssler, M., Weisshaar, E.: 1984a, *Astron. Astrophys.* **139**, 426
Deinzer, W., Hensler, G., Schüssler, M., Weisshaar, E.: 1984b, *Astron. Astrophys.* **139**, 435
Dravins, D., Larsson, B.: 1984, in *Small-Scale Dynamical Processes in Quiet Stellar Atmospheres*, ed. S.L. Keil, Sacramento Peak, NM, USA, p. 306
Frazier, E.N., Stenflo, J.O.: 1972, *Solar Phys.* **27**, 330
Frazier, E.N., Stenflo, J.O.: 1978, *Astron. Astrophys.* **70**, 789
Gingerich, O., Noyes, R.W., Kalkofen, W., Cuny, Y.: 1971, *Solar Phys.* **18**, 347
Grossmann-Doerth, U., Knölker, M. Schüssler, M.: 1989, in *Solar and Stellar Granulation*, NATO Advanced Research Workshop, eds. R.J. Rutten, G. Severino, Reidel, Dordrecht, p. 481
Grossmann-Doerth, U., Larsson, B., Solanki, S.K.: 1988a, *Astron. Astrophys.* **204**, 266
Grossmann-Doerth, U., Schüssler, M., Solanki, S.K.: 1988b, *Astron. Astrophys.* **206**, L37
Gustafsson, B.: 1973, *Uppsala Astron. Obs. Ann.* **5**, No. 6
Harvey, J.W., Livingston, W.: 1969, *Solar Phys.* **10**, 283
Hirayama, T.: 1978, *Publ. Astron. Soc. Japan* **30**, 337
Holweger, H., Müller, E. A.: 1974, *Solar Phys.* **39**, 19
Holweger, H.: 1979, in *Proc. 22nd Liège International Astrophys. Symp.*, Inst. d'Astrophysique, Liège, 117
Howard, R.W., Stenflo, J.O.: 1972, *Solar Phys.* **22**, 402
Kalkofen, W., Bodo, G., Massaglia, S., Rossi, P.: 1989, in *Solar and Stellar Granulation*, NATO Advanced Research Workshop, eds. R.J. Rutten, G. Severino, Reidel, Dordrecht, p. 571
Keller, C.U.: 1990, in *Solar Photosphere: Structure, Convection, Magnetic Fields*, ed. J.O. Stenflo, IAU Symp. **138**, Kiev, p. 121
Knölker, M., Schüssler, M.: 1988, *Astron. Astrophys.* **202**, 275
Knölker, M., Schüssler, M., Weisshaar, E.: 1985, in *Theoretical Problems in High Resolution Solar Physics*, ed. H.U. Schmidt, Max-Planck-Institut für Astrophysik, Munich, p. 195
Koutchmy, S., Stellmacher, G.: 1978, *Astron. Astrophys.* **67**, 93
Kroll, S., Kock, M.: 1987, *Astron. Astrophys. Suppl. Ser.* **67**, 225
Landi Degl'Innocenti, E., Landolfi, M.: 1982, *Solar Phys.* **77**, 13
Marquardt, D.W.: 1963, *J. Soc. Ind. Appl. Math.* **11**, 431
Mein, P., Mein, N., Malherbe, J.M.: 1985, in *Theoretical Problems in High Resolution Solar Physics*, ed. H.U. Schmidt, Max-Planck-Institut für Astrophysik, Munich, p. 303
Mihalas, D.: 1978, *Stellar Atmospheres*, Freeman, San Francisco
Moity, J.: 1983, *Astron. Astrophys. Suppl. Ser.* **52**, 37
Muller, R.: 1975, *Solar Phys.* **45**, 105
Muller, R., Keil, S.L.: 1983, *Solar Phys.* **87**, 243
Pantellini, F.G.E., Solanki, S.K., Stenflo, J.O.: 1988, *Astron. Astrophys.* **189**, 263
Parker, E.N.: 1979, *Astrophys. J.* **230**, 905
Pauls, U., Grevesse, N., Huber, M.C.E.: 1990, *Astron. Astrophys.* (submitted)
Rees, D.E., Murphy, G.A., Durrant, C.J.: 1989, *Astrophys. J.* **339**, 1093
Roberts, B., Webb, A.R.: 1978, *Solar Phys.* **56**, 5
Rogerson, J.B.: 1961, *Astrophys. J.* **134**, 331
Rutten, R.J., Kostik, R.I.: 1982, *Astron. Astrophys.* **115**, 104
Schüssler, M.: 1983, in *Solar and Stellar Magnetic Fields: Origins and Coronal Effects*, ed. J.O. Stenflo, IAU Symp. **102**, 213
Schüssler, M.: 1986, in *Small Scale Magnetic Flux Concentrations in the Solar Photosphere*, eds. W. Deinzer, M. Knölker, H.H. Voigt, Vandenhoeck & Ruprecht, Göttingen, p. 103
Schüssler, M.: 1987, in *Proc. Workshop on the Role of Fine-Scale Magnetic Fields on the Structure of the Solar Atmosphere*, eds. E.H. Schröter, M. Vázquez, A.A. Wyller, Cambridge University Press, Cambridge, p. 223
Schüssler, M.: 1990, in *Solar Photosphere: Structure, Convection, Magnetic Fields*, ed. J.O. Stenflo, IAU Symp. **138**, Kiev, p. 161
Schüssler, M., Solanki, S.K.: 1988, *Astron Astrophys.* **192**, 338
Skumanich, A., Lites, B.W.: 1987, *Astrophys. J.* **322**, 473
Smith, M.A., Testerman, L., Evans, J.C.: 1976, *Astrophys. J.* **207**, 308
Sobotka, M.: 1989, *Solar Phys.* **124**, 37
Solanki, S.K.: 1984, in *The Hydromagnetics of the Sun*, eds. T.D. Guyenne, J.J. Hunt, Proc. Fourth European Meeting on Solar Physics, ESA SP-220, p. 63
Solanki, S.K.: 1986, *Astron. Astrophys.* **168**, 311
Solanki, S.K.: 1987, Ph.D. Thesis, ETH Zürich
Solanki, S.K.: 1989, *Astron. Astrophys.* **224**, 225
Solanki, S.K.: 1990, in *Solar Photosphere: Structure, Convection, Magnetic Fields*, ed. J.O. Stenflo, IAU Symp. **138**, Kiev, p.103
Solanki, S.K., Biémont, E., Mürset, U.: 1990, *Astron. Astrophys. Suppl. Ser.* (in press)
Solanki, S.K., Keller, C., Stenflo, J.O.: 1987, *Astron. Astrophys.* **188**, 183
Solanki, S.K., Steenbock, W.: 1988, *Astron. Astrophys.* **189**, 243
Solanki, S.K., Stenflo, J.O.: 1984, *Astron. Astrophys.* **140**, 185
Solanki, S.K., Stenflo, J.O.: 1985, *Astron. Astrophys.* **148**, 123
Solanki, S.K., Stenflo, J.O.: 1986 *Astron. Astrophys.* **170**, 120
Spruit, H.C.: 1976, *Solar Phys.* **50**, 269
Spruit, H.C.: 1977, *Solar Phys.* **55**, 3
Spruit, H.C.: 1981, in *The Physics of Sunspots*, eds. L.E. Cram, J.H. Thomas, Sacramento Peak, NM, USA, p. 98
Spruit, H.C., Roberts, B.: 1983, *Nature* **304**, 401
Steiner, O.: 1990, *Astron. Astrophys.* (in press)
Steiner, O., Pizzo, V.J.: 1989, *Astron Astrophys.* **211**, 447
Steiner, O., Pneumann, G.W., Stenflo, J.O.: 1986, *Astron. Astrophys.* **170**, 126
Steiner, O., Stenflo, J.O.: 1990, in *Solar Photosphere: Structure, Convection, Magnetic Fields*, ed. J.O. Stenflo, IAU Symp. **138**, Kiev, p.181
Stellmacher, G., Wiehr, E.: 1979, *Astron. Astrophys.* **75**, 263
Stenflo, J.O.: 1973, *Solar Phys.* **32**, 41

Stenflo, J.O.: 1975, *Solar Phys.* **42**, 79
Stenflo, J.O.: 1976, in *Basic Mechanisms of Solar Activity*, eds. V. Bumba, J. Kleczek, IAU Symp. **71**, p. 69
Stenflo, J.O.: 1989, *Astron. Astrophys. Rev.* **1**, 3
Stenflo, J.O., Harvey, J.W.: 1985, *Solar Phys.* **95**, 99
Stenflo, J.O., Harvey, J.W., Brault, J.W., Solanki, S.K.: 1984, *Astron. Astrophys.* **131**, 33
Stenflo, J.O., Lindegren, L.: 1977, *Astron. Astrophys.* **59**, 367
Stenflo, J.O., Solanki, S.K., Harvey, J.W.: 1987, *Astron. Astrophys.* **171**, 305
Stenholm, L.G., Stenflo, J.O.: 1978, *Astron. Astrophys.* **67**, 33
Thévenin, F.: 1989, *Astron. Astrophys. Suppl. Ser.* **77**, 137
Title, A.M., Tarbell, T.D., Topka, K.P., Ferguson, S.H., Shine, R.A. and the SOUP team: 1989, *Astrophys. J.* **336**, 475
Van Ballegooijen, A.A.: 1984, *Solar Phys.* **91**, 195
Van Ballegooijen, A.A.: 1985, in *Theoretical Problems in High Resolution Solar Physics*, ed. H.U. Schmidt, Max-Planck-Institut für Astrophysik, Munick, p. 177
Vernazza, J.E., Avrett, E.H., Loeser, R.: 1976, *Astrophys. J. Suppl. Ser.* **30**, 1
Walton, S.R.: 1987, *Astrophys. J.* **312**, 909
Wilson, P.R.: 1971, *Solar Phys.* **21**, 101
Zayer, I., Solanki, S.K., Stenflo, J.O.: 1989, *Astron. Astrophys.* **211**, 463